HIGH FREQUENCY ULTRASOUND IMAGING OF CHANGES IN CELL STRUCTURE INCLUDING APOPTOSIS

R.E. Baddour[1*], M.D. Sherar[1,2], G.C. Czarnota[2,3], J.W. Hunt[1],
L. Taggart[2], A. Giles[2], N.R. Farnoud[3], and M.C. Kolios[1,3]

[1]Dept. of Medical Biophysics, University of Toronto, 610 University Avenue, Toronto, ON, M5G2M9, Canada
[2]Ontario Cancer Institute, Princess Margaret Hospital, 610 University Avenue, Toronto, ON, M5G2M9, Canada
[3]Dept. of Mathematics, Physics and Computer Science, Ryerson University,
350 Victoria Street, Toronto, ON, M5B2K3, Canada

Abstract – It has been previously shown that high frequency ultrasound (20 - 100 MHz) can be used to detect cellular structure changes in tissues and cell ensembles. Using spectral analysis methods to analyze radio-frequency data collected from in vitro and in vivo models, the changes seen during apoptotic cell death are very striking. Imaging changes in cell structure has implications in a broad range of fields, from cancer treatment monitoring to organ transplantation. However, the changes seen in the backscattered ultrasound intensity and frequency spectrum are not fully understood. In this paper we propose and explore a model for studying how the changes in the sizes, spatial distribution, and acoustic impedance of the scattering sources within the cells are related to the resulting backscattered ultrasound signal.

I. INTRODUCTION

During the last 15 years, several studies have found that localized cellular variations in tissues [1, 2] and cell ensembles [3, 4] can be detected using high frequency ultrasound (20 - 100 MHz). Although individual cells cannot be resolved even at the high frequencies used, changes in the localized brightness and speckle in conventional B-mode images can readily be observed. More recently, spectral analysis techniques [5, 6] used to analyze radio-frequency (RF) echo signals, have made it possible to more specifically characterize cell structure changes in tissues [7] and cell ensembles [8].

Several types of changes in cell structure have been successfully detected in vitro using high frequency ultrasound. In particular, we have looked extensively at changes in structure of human acute myeloid leukemia cells, OCI-AML-5 [9], that occur after exposure to increased salinity, during necrosis, and during apoptosis. We have shown [10] that exposing cells to higher ionic strengths, which induces cell shrinkage and condensed chromatin distributed throughout the cell nucleus, increases the ultrasound backscatter of cell ensembles. We have also shown that ensembles of necrotic cells (heat killed) [11], cells undergoing mitosis [8], and cells undergoing apoptosis (after exposure to cisplatin, a commonly used chemotherapeutic agent) [8, 11] yield an increased ultrasound backscattered signal compared to viable cells. Apoptosis, a process marked by cell and nucleus shrinkage, complete condensation of chromatin in the nucleus, and eventual nuclear fragmentation [12], causes the most dramatic increase in high frequency ultrasound scattering; up to a 20-fold change in integrated backscatter intensity compared to viable cells [8].

Apoptosis is now recognized to be a central feature in embryonic development [13, 14], certain neurodegenerative disorders [15], and cancer [16, 17]. Apoptosis can be induced by disease, such as in transplant rejection [18] or heart attack [19], or can be purposefully induced as the result of cancer therapy [20, 21]. Because apoptosis is a biologically significant process, we have made high frequency ultrasound measurements ex vivo and in vivo to determine whether apoptotic changes can be detected in experimental organ and tumor systems.

Apoptosis occurs in organs due to ischemia during isolation and storage prior to transplantation. It has been shown in rat liver that the degree of endothelial cell injury correlates with functional impairment of

the organ following transplantation [22]. Measurement of organ damage by detecting apoptosis might allow assessment of the viability of organs prior to transplantation. Measurement of apoptosis would also be useful for assessing new organ preservation techniques which aim to inhibit apoptosis [23]. We have performed studies in excised mouse liver to test the feasibility of monitoring organ viability using high frequency ultrasound. Using a high frequency ultrasound imager built in-house [3], an increase in image brightness (seen in Figures 1A and 1B) and RF spectral slope (seen in Figure 1C) with time, consistent with ultrasonic features detected from ensembles of pure apoptotic OCI-AML-5 cells [8], was observed. The classic markers of apoptotic cells in spectral analysis are an increase in spectral slope and midband fit.

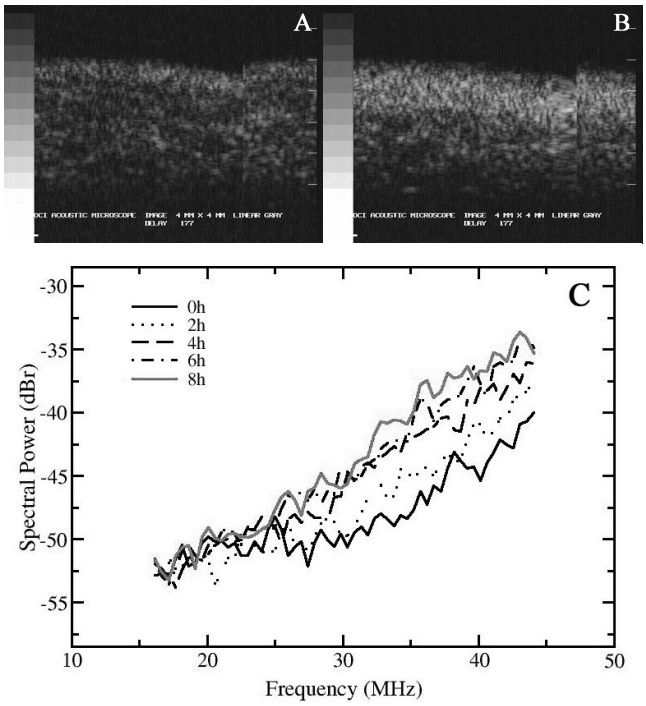

Figure 1: Ultrasonic B-mode images of a mouse liver, approximately 4x3 mm in size, (A) immediately after excision and (B) 8 hours after excision, over the exact same region. In (C), normalized spectral power (in dBr) as a function of frequency for an average of 40 independent RF lines are presented.

Evaluation of cancer treatment response currently takes weeks or months as the tumor shrinks. Measuring apoptosis in a tumor volume could provide a method for rapidly measuring response to anticancer therapies since many cancer treatments including radiation therapy [24], chemotherapy [25], and immunotherapy [26], kill tumor cells by apoptosis. We imaged human tumors grown in mice which were then treated with various cancer therapies to test the feasibility of monitoring anticancer treatment with high frequency ultrasound. In one set of experiments, we treated mice with human malignant melanoma, ATCC HTB-67 [27], tumors with photodynamic therapy (using photofrin photosensitizer and 120 J delivered of 635 nm laser light). Using a VisualSonics VS40b (VisualSonics Corp., Toronto, Canada) ultrasound imaging device operating at 40 MHz, we were able to see edema early on with a bright region in the treated tumor area (4 hour time point shown in Figure 2). At 26 hours, the edema had almost disappeared and a very bright region was observed in the treated area.

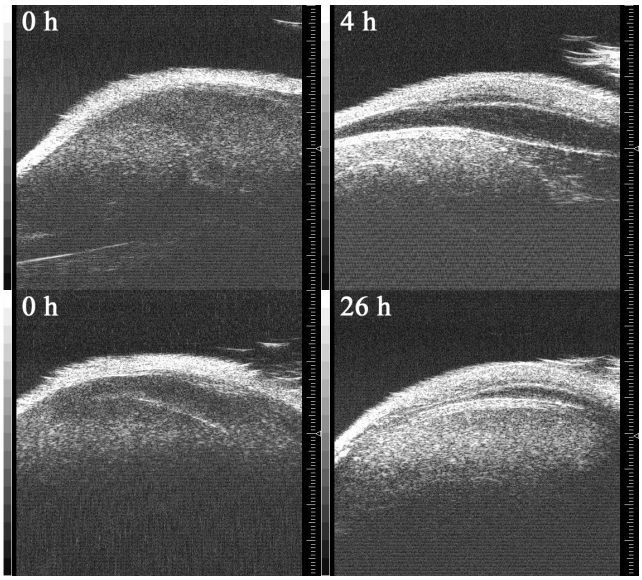

Figure 2: Ultrasonic B-mode images of human malignant melanoma tumors grown in mice (each row is a different mouse), immediately before laser irradiation during photodynamic treatment (0 h), and at two different time points after treatment.

II. PROBLEMS

Presently it is not possible, using image analysis of B-mode images or spectral analysis of RF signals, to measure the proportion of cells in a volume undergoing structural changes. In the case of apoptosis this is referred to as the apoptotic index; the percentage of cells undergoing apoptosis. We have demonstrated that it is possible to non-invasively detect cells undergoing apoptotic changes in vitro, ex

vivo, and in vivo, but we cannot make an accurate assessment of the apoptotic index.

Although RF spectral parameters can be used in an existing theoretical model, such as the one proposed by Lizzi et al. [28, 29], to predict features of the scatterer microstructure, these models assume a random scatterer distribution. This assumption likely does not hold for either cell ensembles or tissues. Cells in tissues may be better modeled as spatially ordered with some degree of randomization. Therefore, calculations of the effective scatterer sizes based on methods assuming completely random distribution are probably inaccurate. It would be useful to know what the acoustic scattering centers are in cells at high frequencies so that we can understand the changes in backscatter intensities following changes in cell structure.

III. ENSEMBLE SCATTERING MODELS

If an ultrasound scattering model can be constructed to simulate an ensemble of cells, with a variable number undergoing apoptosis, it might be possible to solve the problem of calculating the apoptotic index from measured RF spectral parameters. This solution would require empirical calibration for each particular cell type. As a starting point, we have chosen to model in vitro cell ensembles of OCI-AML-5 cells. These cells are conveniently spherical in shape with relatively spherical nuclei.

The differences in backscatter intensities observed following changes in cell structure can be due to changes in the ultrasonic cellular properties (and, hence, of the subcellular scattering sources) or be related to the spatial arrangement of the scattering sources. It is probable that both factors are important. For example, if a cell's diameter is reduced, the number of possible positions of the nucleus is reduced because the nucleus will take up a larger proportion of the cell volume. A reduced cell diameter will also have consequences for the spatial packing of cells in an ensemble.

Existing ensemble model

Although the primary scattering centers of a cell are unknown, the evidence presented to date [8, 30, 31] indicate that the cell nucleus is the predominant scatterer. Based on this assumption, a simple model of a cell ensemble can be constructed. Hunt et al. [32] carried out two-dimensional simulations for regular and pseudo-random distributions of cells, each containing a single weak pseudo-point scatterer (i.e. not a Rayleigh point scatterer) fixed in the centre of the cell simulating the nucleus. Hunt et al. [32] showed that as the randomization of the position of the cells (and, thus, the nuclei) increases, the calculated backscattered signals also increases. A recent refinement of this model [33] now employs multiple pseudo-point scatterers arranged to mimic the size and position of the nucleus inside the cell. Several simulations were carried out to model the changes that occur to the nucleus during apoptosis. An increase in the backscatter was predicted as the nucleus size decreases. A further increase in backscatter is predicted in late apoptosis as the nucleus fragments. This trend of increasing backscatter over time agrees with the results our previous studies of cell ensembles imaged at different time points after an apoptotic-inducing treatment [8, 11, 30].

The model developed by Hunt et. al. [32, 33] assumes a very simplified scattering function; the incident pulse is scaled and inverted by each scatterer. As a result, there is no appreciable frequency response associated with the backscatter signal. We have shown [8] that there is an increase in higher frequency backscatter from ensembles of apoptotic cells when compared to viable cells. Therefore, to fully describe these variations in backscatter, a true ensemble scattering model must be constructed.

New ensemble model

We have developed a new two-dimensional ensemble scattering model based on the Faran-Hickling solution [34, 35] of the acoustic scattering field for a compressible sphere (of any diameter, density, speed of sound, and Poisson's ratio) insonified by a plane wave of arbitrary frequency. This scattering solution, an extension of Mie scattering theory [36], has no assumptions regarding scatterer size and is valid for any scatterer diameter. The theoretical response of our model, from an ensemble of cells with spherical nuclei as the sole scatterers, is calculated by summing the equivalent backscattered pressure pulses generated from each nucleus (accordingly time-delayed by depth) weighted by a transducer aperture function. The equivalent scattered pulse from each nucleus is determined by taking the inverse Fourier Transform

of the impulse response of the backscattered pressure calculated using the Faran-Hickling solution of acoustic scattering.

Like the Hunt et al. [32] ensemble model, the spatial arrangement of cells in the ensemble can be varied, for example, to simulate perfect, crystal-like close-packing or more random cell arrangements (see Figure 3). To mimic backscattering from real cell ensembles it is necessary to measure their packing arrangement experimentally. We are currently attempting to extract packing statistics from cell ensembles imaged by confocal optical microscopy.

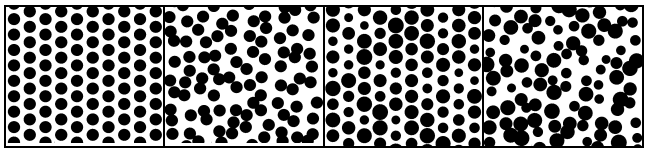

Figure 3: A few possible cell ensemble packings (only cell nuclei are shown). From left: perfect crystal, cell locations are allowed a degree of randomization, nucleus diameters are allowed a degree of randomization, both cell locations and nucleus diameters are randomized.

Unlike Hunt et al. [33], we can now not only vary the dimensions, but also the acoustic properties (density, speed of sound, Poisson's ratio) of any individual nucleus in the ensemble. To simulate a change in cell structure, such as apoptosis, these properties are varied accordingly. Figure 4 shows the effect of diameter and speed of sound (holding density constant) on the backscatter response of a single simulated nucleus. To simulate early stage apoptosis the nucleus diameter would be reduced, and the density and speed of sound would be most likely be increased. It is unknown if the average Poisson's ratio of the nucleus would change during apoptosis. Clearly, to get meaningful results that we can compare to our experimental studies of OCI-AML-5 cell ensembles, we need to make accurate measurements of the acoustic properties of viable and apoptotic OCI-AML-5 nuclei (ideally at several stages of apoptosis).

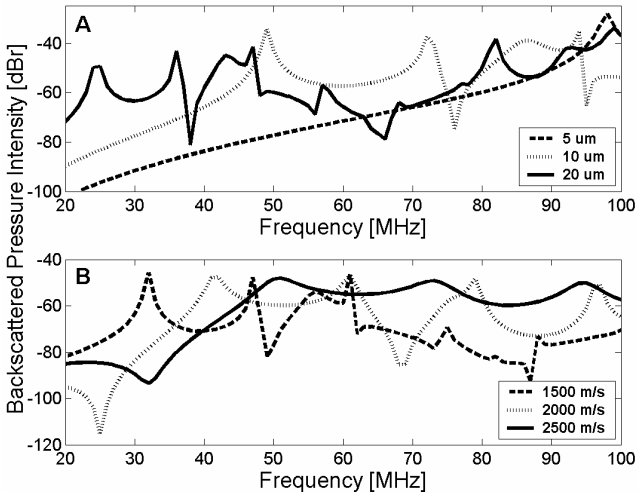

Figure 4: Normalized backscattered pressure intensity from a single spherical scatterer in water. (A) Diameter is varied; density (1.05 g/mL), speed of sound (1540 m/s), and Poisson's ratio (0.33) are kept constant. (B) Compressibility is varied (by varying the speed of sound); density (1.05 g/mL), diameter (15 μm), and Poisson's ratio (0.33) are kept constant.

Some pilot size measurements of viable and early-apoptotic OCI-AML-5 cells were performed using a confocal microscope. The cells were stained with bisbenzimide (Hoescht) and carboxyfluorescein succinimidyl ester (CFSE) to visually segment nucleus and cell membrane respectively. Viable nuclei were, on average, 11 μm in diameter, and early-apoptotic nuclei were 9 μm. Viable cells had a diameter of roughly 14 μm. Changes in apoptotic cell diameter could not be properly assessed due to reduced CFSE dye adherence. This might be due to a change in membrane polarity during apoptosis. [37]

We are also currently in the process of measuring the acoustic parameters of whole nuclei from viable and apoptotic OCI-AML-5 cells. The method of Rill et al. [38] is used to isolate whole undamaged nuclei from cells. At the time of this publication, the only preliminary measurement completed is the speed of sound of viable nuclei: 1584 m/s. This is higher than the average value for soft tissue of 1540 m/s [39, 40]. Because of chromatin condensation and a reduction in diameter, we predict that nuclei from apoptotic cells will have an even higher speed of sound.

IV. NEW ENSEMBLE MODEL RESULTS

As we do not yet know the acoustic properties of OCI-AML-5 cell nuclei, the effect of the spatial arrangement of the cells was explored first. Nuclei, since modeled to be centrally positioned inside cells, have a spatial arrangement directly related to cells. In the model, the variable *cellLocRange* controls the randomness of the cell positions in an ensemble. When *cellLocRange* is zero, the cells and nuclei are packed in a perfect lattice. As *cellLocRange* (defined as a fraction of the average cell diameter) increases, cells are allowed to randomly take positions farther away from their assigned lattice position. Assuming

some reasonable nuclei properties (see Figure 5), simulations were performed for different values of *cellLocRange*. The midband fit and spectral slope, as defined in [28], of the resulting backscattered signals are presented in Figure 5. It is encouraging that the range of spectral slopes generated by the simulations are close to values measured experimentally from OCI-AML-5 cell ensembles (see [8]).

As predicted by Hunt et al. [32], the integrated backscatter, and hence the midband fit, is at a minimum when cells are in a perfect lattice. As randomization of cell positions increases, midband fit and spectral slope increase up to a terminal value. The terminal value is achieved when the scatterers, the nuclei, become truly randomly distributed. True random distribution of scatterers appears to occur when *cellLocRange* > 1.25.

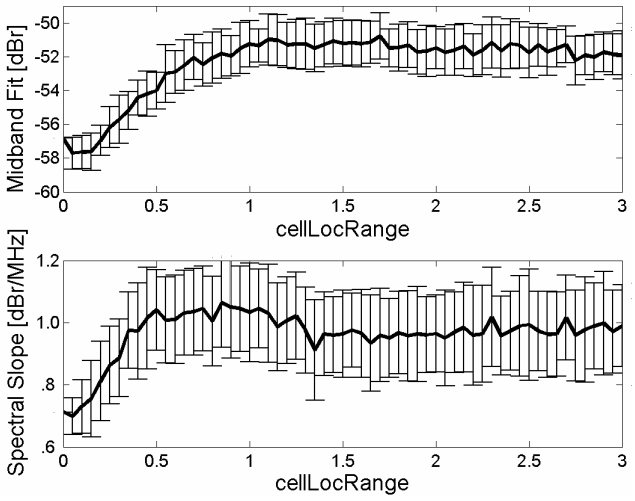

Figure 5: Linear spectral parameters (calculated for the band 25-55 MHz) of simulated normalized backscattered signals from cell ensembles with varying randomness of spatial positions. Each data point is the mean value from 50 cell ensembles; error bars indicate one standard deviation. Assumed nuclear properties: diameter = 15 µm, density = 1.05 g/mL, speed of sound = 1540 m/s, and Poisson's ratio = 0.33.

V. CONCLUSIONS

A new cell ensemble scattering model has been developed. Once we complete the measurement of acoustic properties of viable and apoptotic OCI-AML-5 cells, it will be possible to run exhaustive simulations of various dilutions of apoptotic cells. By comparing these results to experimentally measured RF spectral parameters, we can attempt to deduce the apoptotic index of arbitrary OCI-AML-5 cell ensembles.

ACKNOWLEDGEMENTS

The authors would like to acknowledge the financial support of the Canada Foundation for Innovation, the Canadian Institutes of Health Research, the Natural Sciences and Engineering Research Council of Canada, and the Ontario Innovation Trust.

REFERENCES

[1] G. R. Lockwood, et al., "Invitro High-Resolution Intravascular Imaging in Muscular and Elastic Arteries," *J. Am. Coll. Cardiol.*, vol. 20, pp. 153-160, 1992.

[2] C. J. Pavlin, et al., "Clinical use of ultrasound biomicroscopy," *Ophthalmology*, vol. 98, pp. 287-295, 1991.

[3] M. D. Sherar, et al., "Ultrasound Backscatter Microscopy Images the Internal Structure of Living Tumor Spheroids," *Nature*, vol. 330, pp. 493-495, 1987.

[4] L. R. Berube, et al., "Use of a High-Frequency Ultrasound Microscope to Image the Action of 2-Nitroimidazoles in Multicellular Spheroids," *Br. J. Cancer*, vol. 65, pp. 633-640, 1992.

[5] E. J. Feleppa, et al., "Diagnostic Spectrum Analysis in Ophthalmology - a Physical Perspective," *Ultrasound Med. Biol.*, vol. 12, pp. 623-631, 1986.

[6] F. L. Lizzi, et al., "Statistical framework for ultrasonic spectral parameter imaging," *Ultrasound Med. Biol.*, vol. 23, pp. 1371-1382, 1997.

[7] C. Guittet, et al., "In vivo high-frequency ultrasonic characterization of human dermis," *IEEE Trans. Biomed. Eng.*, vol. 46, pp. 740-746, 1999.

[8] M. C. Kolios, et al., "Ultrasonic spectral parameter characterization of apoptosis," *Ultrasound Med. Biol.*, vol. 28, pp. 589-597, 2002.

[9] C. Wang, et al., "Mast-Cell Growth-Factor, a Ligand for the Receptor Encoded by C-Kit, Affects the Growth in Culture of the Blast Cells of Acute Myeloblastic-Leukemia," *Leukemia*, vol. 5, pp. 493-499, 1991.

[10] M. C. Kolios, et al., "Analysis of Ultrasound Backscatter from Ensembles of Cells and Isolated Nuclei," in *Proc. IEEE Ultrason. Symp.*, 2001, pp. 1257-1260.

[11] G. J. Czarnota, et al., "Ultrasonic biomicroscopy of viable, dead and apoptotic cells," *Ultrasound Med. Biol.*, vol. 23, pp. 961-965, 1997.

[12] G. Hacker, "The morphology of apoptosis," *Cell Tissue Res.*, vol. 301, pp. 5-17, 2000.

[13] M. Watanabe, et al., "Apoptosis is required for the proper formation of the ventriculo-arterial connections," *Dev. Biol.*, vol. 240, pp. 274-288, 2001.

[14] D. Nijhawan, et al., "Apoptosis in neural development and disease," *Annu. Rev. Neurosci.*, vol. 23, pp. 73-87, 2000.
[15] D. Offen, et al., "Apoptosis as a general cell death pathway in neurodegenerative diseases," *J. Neural Transm.-Suppl.*, pp. 153-166, 2000.
[16] R. Strange, et al., "Apoptosis in normal and neoplastic mammary gland development," *Microsc. Res. Tech.*, vol. 52, pp. 171-181, 2001.
[17] A. Bedi, et al., "Inhibition of Apoptosis During Development of Colorectal-Cancer," *Cancer Res.*, vol. 55, pp. 1811-1816, 1995.
[18] S. M. Krams, et al., "Apoptosis as a Mechanism of Cell-Death in Liver Allograft-Rejection," *Transplantation*, vol. 59, pp. 621-625, 1995.
[19] A. Saraste, et al., "Apoptosis in human acute myocardial infarction," *Circulation*, vol. 95, pp. 320-323, 1997.
[20] M. A. Barry, et al., "Activation of Programmed Cell-Death (Apoptosis) by Cisplatin, Other Anticancer Drugs, Toxins and Hyperthermia," *Biochem. Pharmacol.*, vol. 40, pp. 2353-2362, 1990.
[21] J. F. R. Kerr, et al., "Apoptosis - Its Significance in Cancer and Cancer-Therapy," *Cancer*, vol. 73, pp. 2013-2026, 1994.
[22] W. S. Gao, et al., "Apoptosis of sinusoidal endothelial cells is a critical mechanism of preservation injury in rat liver transplantation," *Hepatology*, vol. 27, pp. 1652-1660, 1998.
[23] G. G. Wu, et al., "Antiapoptotic compound to enhance hypothermic liver preservation," *Transplantation*, vol. 63, pp. 803-809, 1997.
[24] R. J. Bold, et al., "Apoptosis, cancer and cancer therapy," *Surg Oncol*, vol. 6, pp. 133-142, 1997.
[25] G. I. Evan and K. H. Vousden, "Proliferation, cell cycle and apoptosis in cancer," *Nature*, vol. 411, pp. 342-348, 2001.
[26] S. Hanada, et al., "Immunotherapy of human colon cancer by antibody-mediated induction of apoptosis," *Gastroenterology*, vol. 110, pp. A525, 1996.
[27] H. F. Oettgen, et al., "Suspension Culture of a Pigment-Producing Cell Line Derived from a Human Malignant Melanoma," *J. Natl. Cancer Inst.*, vol. 41, pp. 827-843, 1968.
[28] F. L. Lizzi, et al., "Theoretical Framework for Spectrum Analysis in Ultrasonic Tissue Characterization," *J. Acoust. Soc. Am.*, vol. 73, pp. 1366-1373, 1983.
[29] F. L. Lizzi, et al., "Comparison of Theoretical Scattering Results and Ultrasonic Data from Clinical Liver Examinations," *Ultrasound Med. Biol.*, vol. 14, pp. 377-385, 1988.
[30] G. J. Czarnota, et al., "Ultrasound imaging of apoptosis: high-resolution non-invasive monitoring of programmed cell death in vitro, in situ and in vivo," *Br. J. Cancer*, vol. 81, pp. 520-527, 1999.
[31] M. C. Kolios, et al., "Ultrasonic spectrum analysis of apoptotic cell populations," *Faseb J*, vol. 13, pp. A1435, 1999.
[32] J. W. Hunt, et al., "The Subtleties of Ultrasound Images of an Ensemble of Cells - Simulation from Regular and More Random Distributions of Scatterers," *Ultrasound Med. Biol.*, vol. 21, pp. 329-341, 1995.
[33] J. W. Hunt, et al., "A model based upon pseudo regular spacing of cells combined with the randomisation of the nuclei can explain the significant changes in high-frequency ultrasound signals during apoptosis," *Ultrasound Med. Biol.*, vol. 28, pp. 217-226, 2002.
[34] J. J. Faran, "Sound Scattering by Solid Cylinders and Spheres," *J. Acoust. Soc. Am.*, vol. 23, pp. 405-418, 1951.
[35] R. Hickling, "Analysis of Echoes from a Solid Elastic Sphere in Water," *J. Acoust. Soc. Am.*, vol. 34, pp. 1582-1592, 1962.
[36] G. Mie, "Beiträge zur Optik trüber Medien, speziell kolloidaler Metallösungen," *Annalen der Physik*, vol. 25, pp. 377-445, 1908.
[37] I. Vermes, et al., "A Novel Assay for Apoptosis - Flow Cytometric Detection of Phosphatidylserine Expression on Early Apoptotic Cells Using Fluorescein-Labeled Annexin-V," *J. Immunol. Methods*, vol. 184, pp. 39-51, 1995.
[38] R. L. Rill, et al., "Isolation and Characterization of Chromatin Subunits," in *Methods in Cell Biology*, vol. 18, *Chromatin and Chromosomal Protein Research III*, G. Stein, J. Stein, and L. J. Kleinsmith, Eds.: Academic Press, 1978, pp. 76-79.
[39] S. A. Goss, et al., "Comprehensive Compilation of Empirical Ultrasonic Properties of Mammalian-Tissues," *J. Acoust. Soc. Am.*, vol. 64, pp. 423-457, 1978.
[40] S. A. Goss, et al., "Compilation of Empirical Ultrasonic Properties of Mammalian-Tissues II," *J. Acoust. Soc. Am.*, vol. 68, pp. 93-108, 1980.

Corresponding author:
* R.E. Baddour, e-mail: rbaddour@uhnres.utoronto.ca